Journal of
Applied
Crystallography
ISSN 0021-8898

Received 19 May 2000
Accepted 3 August 2000

Estimating nanoparticle size from diffraction measurements

B. D. Hall,[a]* D. Zanchet[b,c] and D. Ugarte[c]

[a]Measurement Standards Laboratory of New Zealand, PO Box 31-310, Lower Hutt, New Zealand, [b]Instituto de Física Gleb Wataghin, UNICAMP CP 6165, 13083-970 Campinas SP, Brazil, and [c]Laboratório Nacional de Luz Síncrotron, CP 6192, 13083-970 Campinas SP, Brazil. Correspondence e-mail: b.hall@irl.cri.nz

Nanometre-sized particles are of considerable current interest because of their special size-dependent physical properties. Debye–Scherrer diffraction patterns are often used to characterize samples, as well as to probe the structure of nanoparticles. Unfortunately, the well known 'Scherrer formula' is unreliable at estimating particle size, because the assumption of an underlying crystal structure (translational symmetry) is often invalid. A simple approach is presented here which takes the Fourier transform of a Debye–Scherrer diffraction pattern. The method works well on noisy data and when only a narrow range of scattering angles is available.

1. Introduction

There is currently intense scientific interest in nanometre-sized particles. The chemical and physical properties of such aggregates, comprising only a few hundred atoms, are in a transition region between the bulk and individual atomic or molecular properties. By understanding size-related changes in these systems, it is hoped that advanced new materials can be developed together with a raft of new technologies.

Perhaps the most fundamental of physical properties is structure; the mutual arrangement of atoms in an aggregate. It has been known for some time that noncrystalline structures occur in many materials at sufficiently small sizes. For example, the so-called 'multiply twinned particle' (MTP) structures have been observed in rare gases (Farges *et al.*, 1973, 1986) and are well documented in metal particles (Marks, 1994). MTP structures exhibit fivefold axes of symmetry, which lack the translational symmetry of a crystal structure. They can, however, be thought of as twinned assemblies of crystalline subunits (Yang, 1979).

The analysis of Debye–Scherrer diffraction data from randomly oriented samples of nanoparticles containing MTPs is complicated by the variety of structures and the size-dependent nature of the diffraction pattern (Hall, 2000). In particular, the characteristic size of particles cannot be reliably estimated from the width of 'peaks' by using the Scherrer formula (Guinier, 1994). Difficulties in applying peak-width-based analysis to nanometre-sized particles have been noted by a number of authors (Grigson & Barton, 1967; Briant & Burton, 1975; Lee & Stein, 1987). A selection of calculated diffraction patterns for similar sized models of nanoparticles are shown in Fig. 1. These structure types are typical of the atomic arrangements that can occur in gold and indeed real samples may have several different structures coexisting in the same size range.

The Scherrer formula is derived assuming that a diffraction peak is associated with a family of crystal planes in a size-limited crystal. The existence of MTPs, imperfect face-centred cubic (f.c.c.) structures, or even the high proportion of atoms at the surface of aggregates, means that translational symmetry is not an underlying feature of nanoparticles. Indeed, it is unwise to associate diffraction features with the notion of Bragg peaks from a family of crystal planes: diffraction patterns are better thought of as a superposition of continuous oscillatory functions in reciprocal space, as described by the Debye equation [equation (1) below].

When information on the distribution of particle size is required, alternative measurements are possible: small-angle X-ray scattering (Guinier & Fournet, 1955; Glatter & Krathy, 1982); transmission electron microscopy (TEM) (Granqvist & Buhrman, 1976); mass spectroscopy (Whetten *et al.*, 1996), *etc*.

This paper presents a simple method of estimating nanoparticle size from Debye–Scherrer diffraction data. By taking a Fourier transform of a diffraction pattern, information relating to the average distribution of interatomic distances within aggregates is obtained. No assumption of periodicity need be made and by examining the range of interatomic distances present, the characteristic size of the particles can be estimated. We have found that this approach can be applied to data with fairly severe constraints, such as a restricted range of scattering angles and a high level of experimental noise.

The next section (§2) reviews the Fourier relationship between the profile of a Debye–Scherrer diffraction pattern and the radial distribution function. This section also considers the problems associated with a restricted range of observation of scattering angles, and the effects of noise. After this, §3

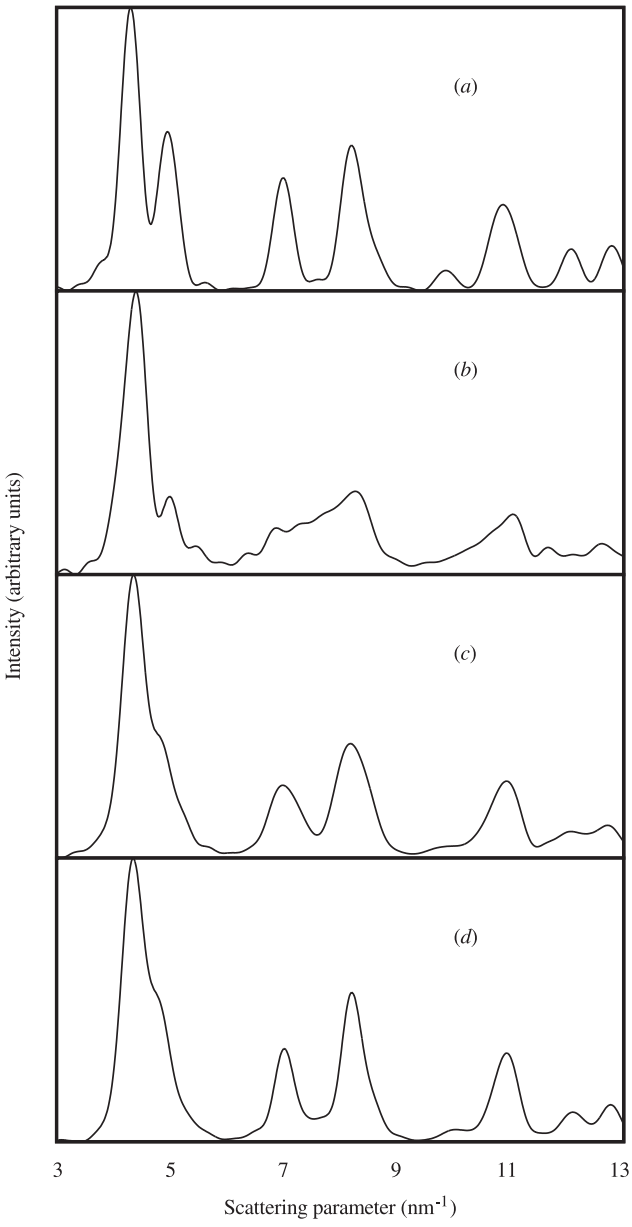

Figure 1
Diffraction patterns of model nanoparticles. Profile (*a*) shows the diffraction pattern of a five-shell f.c.c. particle, approximately 2.8 nm in diameter; profile (*b*) represents a five-shell icosahedral particle, approximately 2.7 nm in diameter; profile (*c*) represents a five-shell truncated decahedron particle, approximately 2.9 nm in diameter; and profile (*d*) shows the diffraction pattern of a small ensemble of imperfect spherical f.c.c. particles. The structures contributing to profile (*d*) have random stacking faults along the [111] direction (with probability 0.3): ten particles were generated in this way and the average of their individual diffraction patterns is shown in (*d*).

presents case studies of the application of this technique: first, to a variety of model (geometric) structures, for which the outcome of the procedure is predictable, and then to X-ray diffraction observations of gold nanoparticles, for which independent TEM observations have been made.

2. The method

The diffracted intensity from a single aggregate is conveniently described by the Debye equation (Guinier, 1994)

$$I_N(s) = I_0 f^2(s)\Big[N + \sum_{n\neq m} \sin(2\pi s r_{mn})/2\pi s r_{mn}\Big], \qquad (1)$$

where I_0 is the incident intensity and $I_N(s)$ is the intensity scattered per unit solid angle in the direction defined by $s = 2\sin(\theta)/\lambda$, with θ equal to half the scattering angle and λ the wavelength of the radiation. The scattering factor, $f(s)$, determines the single-atom contribution to scattering, and is available in tabulated form for most elements and radiations (Wilson, 1992). N is the number of atoms in the cluster and r_{mn} is the distance between atom m and atom n.

In an experimental situation, a sample is characterized by its radial distribution function (r.d.f.), $4\pi r^2\rho(r)$, defined such that $4\pi r^2\rho(r)\,\mathrm{d}r$ is the average number of atom centres with interatomic distances between r and $r + \mathrm{d}r$ (Warren, 1990). The diffracted intensity is then

$$I_N(s) = I_0 f^2(s)\Big\{N + \int_0^\infty 4\pi r^2[\rho(r) - \rho_a]\sin(2\pi s r)/2\pi s r\,\mathrm{d}r\Big\}, \qquad (2)$$

where N is the total number of atoms and ρ_a is the sample average atom density. Nanoparticle samples are usually so dilute that ρ_a is negligible.

The r.d.f. of a model f.c.c. nanoparticle is shown in Fig. 2(*a*). The 'diameter' of this polyhedral structure can be assigned to the largest interatomic distances within the aggregate (about 2.8 nm in this case). Although we do not assume here that it is possible to obtain an experimental r.d.f. of such high resolution, the overall form of the r.d.f. can still be exploited to estimate the particle diameter. This is the motivation underlying the method described below.

In a typical diffraction experiment, a profile of intensity $I^{\exp}(s)$ is recorded over a finite range of s values ($s \in [s_{\min}, s_{\max}]$). Assuming that I_0 and N are unknown, the measured data can be Fourier transformed into real space by calculating

$$P(r) = \beta r \int_{s_{\min}}^{s_{\max}} s[I^{\exp}(s)/\alpha f^2(s) - 1]\sin(2\pi s r)\,\mathrm{d}s, \qquad (3)$$

where α and β are parameters that must be estimated. $P(r)$ is a good approximation to $4\pi r^2\rho(r)$ provided that $s_{\min}$ is very close to zero and $s_{\min}$ is high enough to include most diffraction details. However, this paper is explicitly concerned with cases in which these requirements are not satisfied, and hence in which $P(r)$ differs significantly from $4\pi r^2\rho(r)$ [Figs. 2(*b*) and 2(*c*) are closer to typical].

Fig. 2 suggests how the transformed data may be used to estimate the diameter of the nanoparticle, in spite of the strong oscillations and poor spatial resolution. In Fig. 2(*b*), the decrease in the amplitude of sharp features of $P(r)$ is related to the nearly spherical form of the particle and can be used to estimate the diameter. [Note that scaling values of $P(r)$, *i.e.* $P(r)/\beta$, will not affect this estimate.]

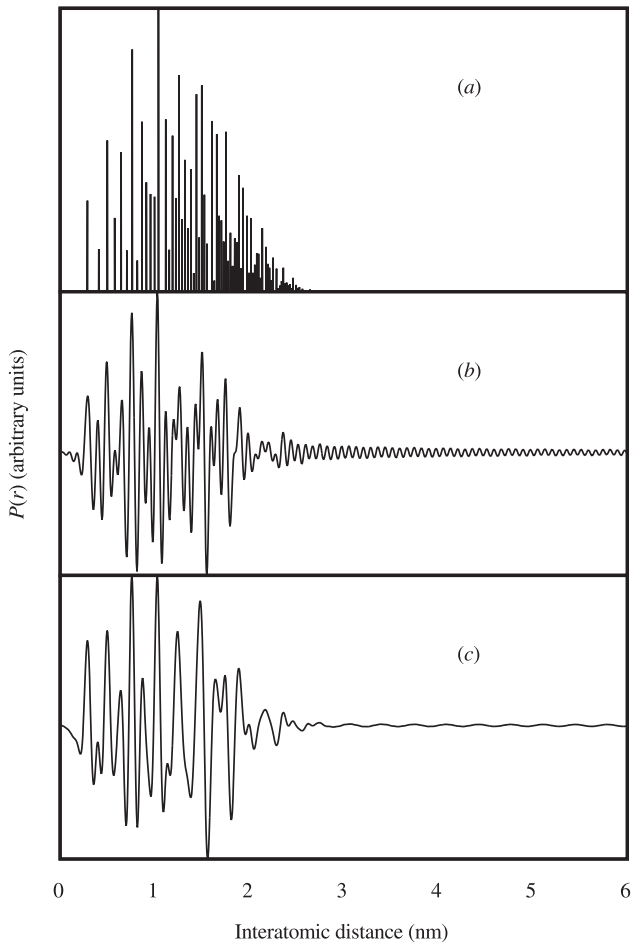

Figure 2
Illustration of how $P(r)$ is related to the wide-angle Debye–Scherrer diffraction pattern shown in Fig. 1(*a*). Curve (*a*) shows the complete r.d.f. of the five-shell (2.8 nm) f.c.c. model particle used in these calculations. Curve (*b*) shows $P(r)$ calculated using the wide-angle data ($s_{\min} = 3$ nm^{-1}, $s_{\min} = 13$ nm^{-1}). Curve (*c*) shows $P(r)$ calculated using the same wide-angle data but including a Lanczos modification function.

An abrupt truncation, caused by the upper limit of diffraction data, will, in general, introduce spurious oscillations in the Fourier transform $P(r)$ (Warren, 1990). These oscillations can extend to higher values of r in $P(r)$, virtually unattenuated (Cohen, 1990), and hence make it difficult to estimate the upper limit of actual interatomic distances in clusters. The problem is more acute if the upper limit of the scattering parameter is reduced and is also exacerbated by measurement noise.

A general approach to the numerical treatment of truncation effects in the inversion of diffraction data has been presented by Waser & Schomaker (1953). The experimental data, obtained in reciprocal space, are weighted with a 'modification function', which will improve the convergence properties of the Fourier transform (hence the alternative name 'convergence factor'). Waser & Schomaker (1953) consider a variety of modification functions, including a pseudo temperature factor, which is also discussed by Warren (1990). In this work, however, we have used a Lanczos function (Hamming, 1986), the appropriate form of which is

$$M(s) = \sin(2\pi sa)/2\pi sa, \tag{4}$$

where $1/a = 2s_{\max}$. Equation (3), for $P(r)$, becomes

$$P(r) = \beta r \int_{s_{\min}}^{s_{\max}} sM(s)[I^{\exp}(s)/\alpha f^2(s) - 1]\sin(2\pi sr)\,\mathrm{d}s. \tag{5}$$

Fig. 2(*c*) shows the considerable improvement brought about by this simple technique. We have found the Lanczos function to be superior to a pseudo temperature modification function: values of the pseudo temperature parameter which provide comparable, or better, attenuation of spurious oscillations in $P(r)$ inevitably result in a loss of resolution compared to the Lanczos function.

Measurement data inevitably include a component of random noise and the effects of this on $P(r)$ are difficult to predict analytically. In this study we have taken a Monte Carlo approach in which independent data sets are generated by adding Poisson noise to raw data, before calculating $P(r)$ [this method has been described more fully by Press *et al.* (1992)]. In this way, the variability of $P(r)$ as a function of r can be examined.

Fig. 3 shows how noise is transformed in $P(r)$. Once again, fairly poor observation conditions have been assumed: the counts recorded at the most intense diffraction peak in the data have been set to 1000. A total of 20 data sets were created using a Poisson random-number generator (Press *et al.*, 1992), for which the average rate at each point was taken from the scaled diffraction pattern. The grey bands in Fig. 3 extend either side of the noise-free line by twice the standard deviation of $P(r)$ values, calculated from the different data sets.

3. Examples

The Fourier method has been applied to two types of diffraction data. First, to a range of model nanoparticles of different internal structures. Then to a series of experimental profiles of thiol-passivated gold nanoparticles, for which independent TEM observations have been made.

3.1. Nanoparticle model structures

Four different nanoparticle models have been used to calculate diffraction patterns (see Fig. 1). In addition to the bulk f.c.c. structure, the two classic MTP structures have been used: the icosahedron (Mackay, 1962; Ino, 1966, 1969) and the truncated decahedron (Bagley, 1965; Ino, 1966, 1969). Also, an ensemble of f.c.c. particles with stacking faults along a [111] direction has been generated by constructing particles as layers of successive (111) planes. At each layer, a stacking fault was introduced with probability 0.3. Spherical boundary conditions were applied to the completed stack to give the required particle size. Ten particles were constructed in this

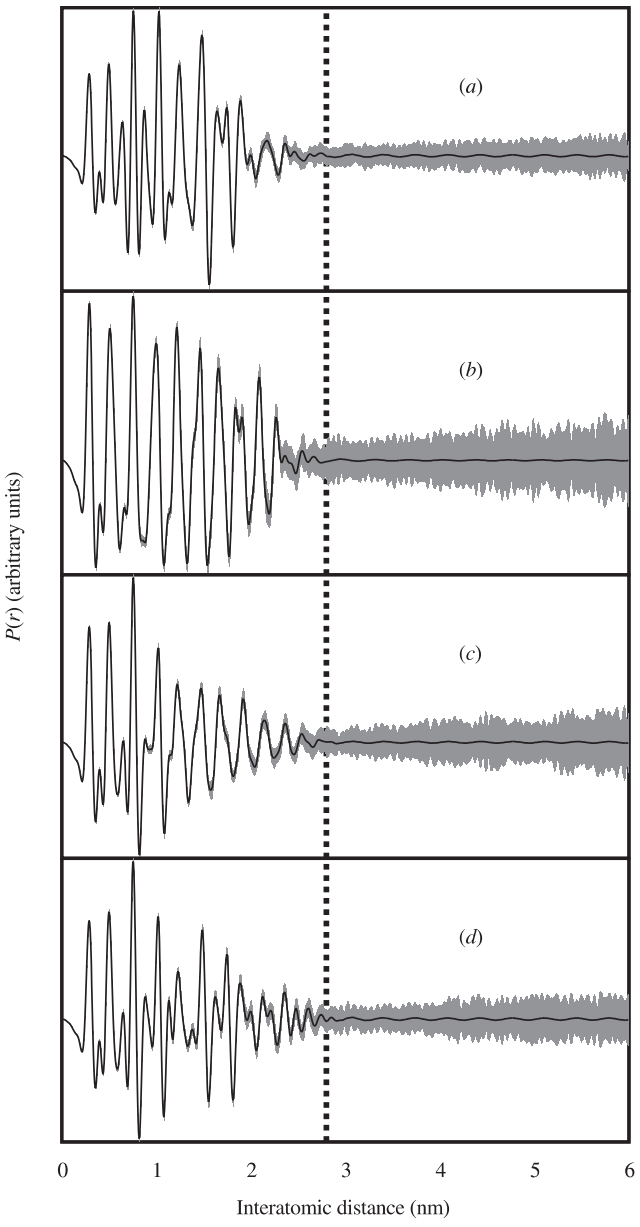

Figure 3
Profiles (*a*) through (*d*) show the results of inverting the diffraction patterns of Fig. 1. In each case, the most intense part of the corresponding diffraction pattern was scaled to approximately 1000 counts and a Poisson random-number generator was used to simulate experimental noise. 20 independent diffraction patterns were generated in this way. The grey bands shown extend to twice the standard deviation of $P(r)$ values calculated from this ensemble. The dotted vertical lines mark the diameter estimated from the exact r.d.f.

way and their average diffraction pattern used as input to the inversion process.

The diameters of the model particles are estimated from the exact r.d.f. of each model: five-shell f.c.c., 2.8 nm; five-shell icosahedron, 2.7 nm; five-shell decahedron 2.9 nm; spherical twinned ensemble, 2.9 nm. These can be compared to values obtained from a crude application of the Scherrer formula, using the main diffraction peak of the corresponding diffraction patterns (noiseless data). One obtains: five-shell f.c.c., 2.4 nm; five-shell icosahedron, 2.0 nm; five-shell decahedron, 1.8 nm; and spherical twinned ensemble, 1.5 nm. On the other hand, from Fig. 3, the noiseless $P(r)$ curves can each be estimated to about ± 0.1 nm of the r.d.f. values. The presence of noise obscures small features in the tail of $P(r)$. This means that the largest distinct feature of $P(r)$ will occur at some value of r less than the diameter. Nevertheless, the trend of decreasing oscillations in $P(r)$ provides a useful guide to the eye, and the graphical banding of the uncertainty arising from the noise provides a good indication of the degree to which small features are likely to be swamped by random fluctuations. Because of this, estimates of the diameter can still be made to within about ± 0.2 nm of the r.d.f. values.

3.2. Gold nanoparticles

A practical example is provided by a series of X-ray diffraction patterns obtained from samples of gold nanoparticles (Zanchet *et al.*, 2000). Three samples were prepared

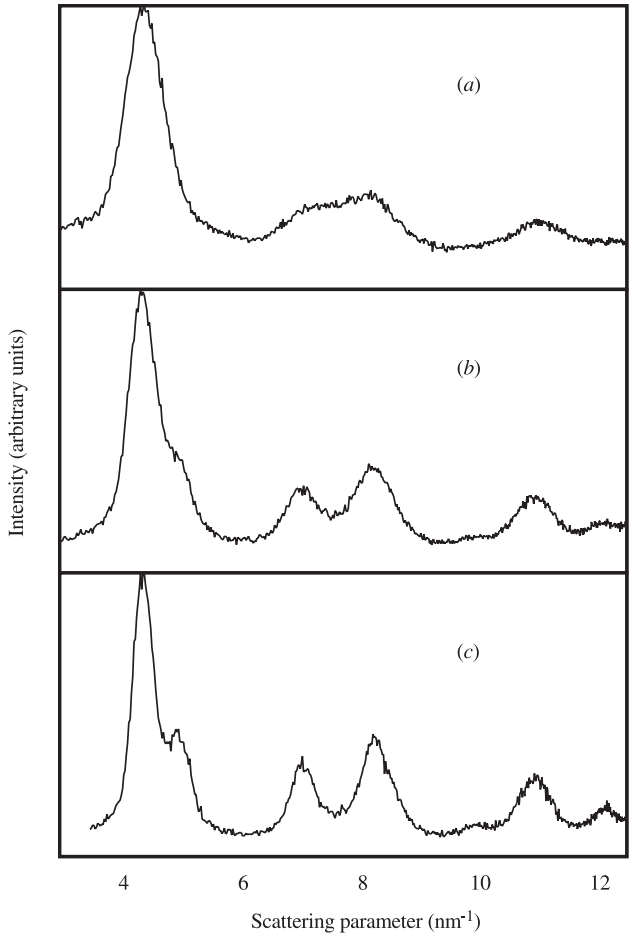

Figure 4
Nanoparticle X-ray diffraction patterns from three different samples of chemically passivated gold particles (Zanchet *et al.*, 2000). The size distributions for profiles (*a*) to (*c*) are shown in Fig. 5.

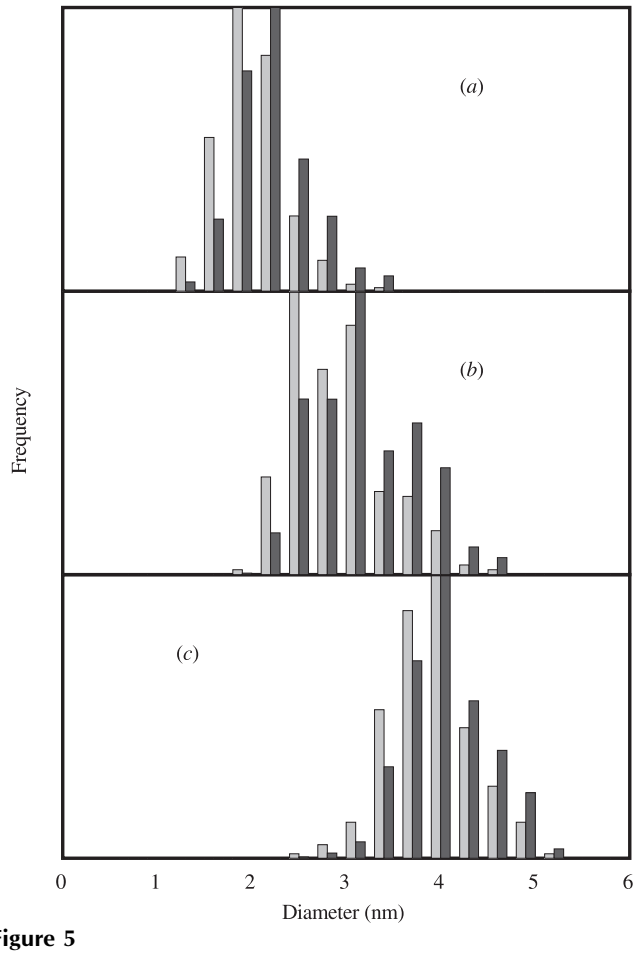

Figure 5
Size distributions obtained from TEM observations of the gold nanoparticle samples from which the diffraction patterns of Fig. 4 were obtained. The direct size distribution is shown with the light grey bars and the volume-weighted size distribution is shown with the dark grey bars. The statistics are: (*a*) 241 particles observed, average diameter ($\overline{d}$) 2.0 nm, volume-weighted average diameter ($\overline{d}_v$) 2.2 nm; (*b*) 217 particles, $\overline{d}$ = 2.9 nm, $\overline{d}_v$ = 3.2 nm; (*c*) 217 particles, $\overline{d}$ = 3.9 nm, $\overline{d}_v$ = 4.1 nm.

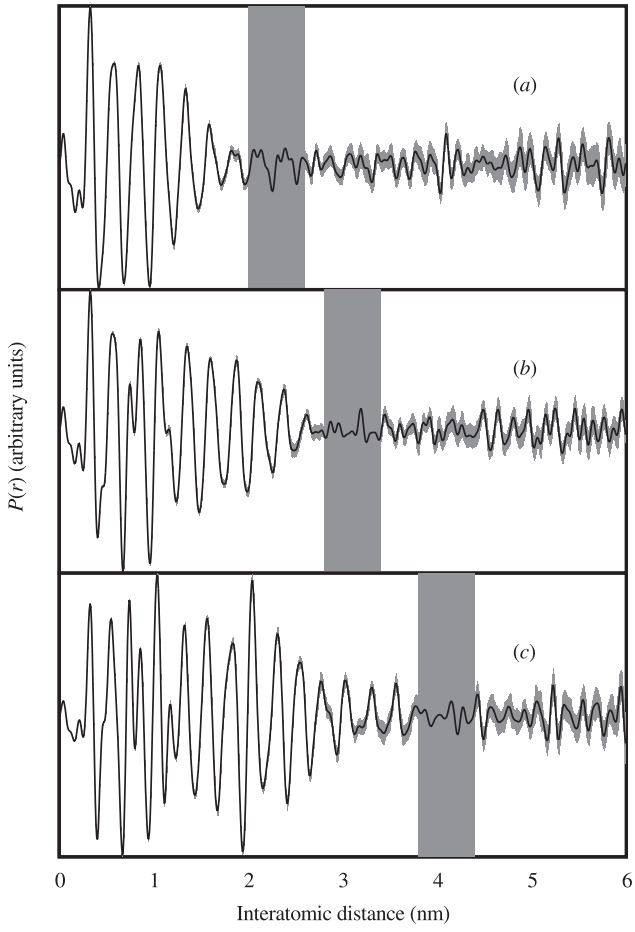

Figure 6
Profiles (*a*) through (*c*) show the results of inverting the diffraction patterns of Fig. 4. The grey noise bands around the $P(r)$ curve were calculated in the same way as Fig. 3, using the actual observed counts to generate suitable data sets. The grey rectangular regions indicate conservative uncertainty intervals around diameter estimates. They are drawn at: (*a*) 2.3 ± 0.3 nm, (*b*) 3.1 ± 0.3 nm, (*c*) 4.1 ± 0.3 nm.

by a wet-chemical synthesis procedure capable of yielding passivated particles in large numbers and with a narrow size distribution. Fig. 4 shows the three corresponding diffraction patterns.

A small number of particles from each sample were also observed by TEM and the sample size distributions are shown in Fig. 5: the direct size distribution, where the frequency is reported as a function of diameter, and volume-weighted distribution, where the volume fraction associated with each histogram bin is reported. The corresponding sample means are, respectively, 2.0, 2.9 and 3.9 nm, by frequency and, 2.2, 3.2 and 4.2 nm by weight. Statistics by weight are included because diffracted intensity is proportional to the number of atoms in a cluster and therefore these statistics are expected better to represent diffraction data from a size-dispersed sample.

To apply the Fourier method to experimental data, the scale factor α of equations (3) and (5) must be estimated. An iterative interactive algorithm is used to refine estimates of α, after inspecting the form of $P(r)$; the process can be repeated until a satisfactory range of values has been identified. The final value of particle size is found to be fairly insensitive to the exact value of α.

Fig. 6 shows the inverted data of the diffraction patterns in Fig. 4. A substrate scattering contribution was subtracted prior to Fourier inversion. This background profile is virtually monotonic and structureless (amorphous glass substrate), so an error in the correction will affect $P(r)$ only at very small values of r. As in Fig. 3, 20 independent diffraction patterns have been calculated using Poisson random noise to generate deviations with respect to the observed data. The grey bands in Fig. 6 show how this noise contributes to the uncertainty in the exact form of $P(r)$. In contrast to Fig. 3, the noise band is smaller around $P(r)$. This reflects the higher numbers of counts in the experimental diffraction patterns. Nevertheless, there is a significant noise component in $P(r)$ and Lanczos

smoothing has considerably reduced the magnitude of fluctuations in the plots.

Fig. 6 shows the relative sizes of the nanoparticles in each sample. The same general progression would have been predicted qualitatively from the narrowing of features in the three corresponding diffraction patterns, shown in Fig. 4. However, detailed analysis of the structure of these samples has shown that they contain a significant fraction of MTP structures (Zanchet *et al.*, 2000). Hence, results obtained by applying the Scherrer formula to this data would be misleading. For example, a rough application of the Scherrer formula to the first maximum of profile (*a*) gives a diameter of only about 1.2 nm!

In Fig. 6, the envelope of decreasing oscillations in $P(r)$ can be extrapolated to identify an upper limit for the interatomic distances of particles in the sample. In this way, a semi-quantitative estimate can be made of the characteristic diameter of the sample. Grey rectangles have been added to Fig. 6, indicating conservative uncertainty for the particle diameters [(*a*) 2.3 $\pm$ 0.3 nm, (*b*) 3.1 $\pm$ 0.3 nm, (*c*) 4.1 $\pm$ 0.3 nm], which agree with the TEM observations of Fig. 5.

4. Discussion and conclusions

There is currently no simple method of estimating nanoparticle size directly from Debye–Scherrer diffraction data. The Scherrer formula cannot be applied to nanoparticle samples, because of overlapping peaks and, more importantly, because of the presence of noncrystalline structures in the samples. These difficulties are avoided by taking a Fourier transform of diffraction data and then making an estimate of particle size. Assuming that diffraction data are available in digital form, the technique is easy to apply.

The Fourier method performs well even when there are quite severe limitations on the range of scattering angles measured, and when noise is important. It provides a semi-quantitative estimate of particle size that is comparable in accuracy with TEM observations, although it does not provide information on the width and shape of the particle size distribution.

The technique will be of value as a complement to established techniques of particle size characterization. For example, it can be used to check the consistency of observations when samples have been handled differently before measurement. The study of gold nanoparticles cited above is a case in point. Samples for observation by TEM and samples for diffraction were prepared separately, although originating from the same batch, and observations were made at different times and under different conditions (vacuum/air), *etc*. Diffraction measurements required a large amount of material, which was compacted and placed on a glass slide, whereas TEM observations used a minute amount from a suspension. The Fourier method provided a useful check that the two preparation methods had not caused the sample characteristics to change (Zanchet *et al.*, 2000).

The technique will also be useful when there is no other convenient means of characterizing particle size. For example, in studies of unsupported nanoparticles (*e.g.* Reinhard, Hall, Berthoud *et al.*, 1997; Reinhard, Hall, Ugarte *et al.*, 1997), in which diffraction patterns of nanoparticles are measured while the particles are completely isolated in a molecular beam and hence free of any support. Although it is sometimes possible to obtain supported samples in these experiments (collected from the beam and later studied by TEM to measure the particle size distribution), the Fourier inversion technique can provide an immediate *in situ* estimate of particle size.

The authors acknowledge the invaluable help of the support staff at LNLS. Electron microscopy was performed at LME/LNLS-Campinas (JEM 3010 ARP), CIME-EPFL, Lausanne (Philips EM430T), and Centro Mic. Eletrônica-UFRGS, Porto Alegre (JEM 2010 ARP). Diffraction measurements were performed on the XRD beamline at the Brazilian Synchrotron Light Facility (LNLS-Campinas, SP). BDH gratefully acknowledges funding under Marsden (98-UOC-042-PSE) and NSOF (N089134), and travel assistance from the Royal Society of New Zealand (00-BRAP-11-HALL). DU and DZ are grateful for financial support from CNPq and FAPESP (Proc. 96/12550-9, 97/04236-4).

References

Bagley, B. G. (1965). *Nature (London)*, **208**, 674–675.
Briant, C. L. & Burton, J. J. (1975). *Surf. Sci.* **51**, 345–351.
Cohen, J. B. (1990). *Ultramicroscopy*, **34**, 41–46.
Farges, J., de Feraudy, M. F., Raoult, B. & Torchet, G. (1986). *J. Chem. Phys.* **84**, 3491–3501.
Farges, J., Raoult, B. & Torchet, G. (1973). *J. Chem. Phys.* **59**, 3454–3458.
Glatter, O. & Krathy, O. (1982). *Small-Angle X-ray Scattering.* New York: Academic Press.
Granqvist, C. G. & Buhrman, R. A. (1976). *J. Appl. Phys.* **47**, 2200–2219.
Grigson, C. W. B. & Barton, E. (1967). *Brit. J. Appl. Phys.* **18**, 175–183.
Guinier, A. (1994). *X-ray Diffraction in Crystals, Imperfect Crystals, and Amorphous Bodies.* New York: Dover.
Guinier, A. & Fournet, G. (1955). *Small-Angle Scattering of X-rays.* New York: Wiley.
Hall, B. D. (2000). *J. Appl. Phys.* **87**, 1666–1675.
Hamming, R. W. (1986). *Numerical Methods for Scientists and Engineers.* New York: Dover.
Ino, S. (1966). *J. Phys. Soc. Jpn*, **21**, 346–362.
Ino, S. (1969). *J. Phys. Soc. Jpn*, **27**, 941–953.
Lee, J. W. & Stein, G. D. (1987). *J. Phys. Chem.* **91**, 2450–2457.
Mackay, A. L. (1962). *Acta Cryst.* **15**, 916–918.
Marks, L. D. (1994). *Rep. Prog. Phys.* **57**, 603–649.
Press, W. H., Teukolsky, S. A., Vetterling, W. T. & Flannery, B. P. (1992). *Numerical Recipes in C: The Art of Scientific Computing.* Cambridge University Press.
Reinhard, D., Hall, B. D., Berthoud, P., Valkealahti, S. & Monot, R. (1997). *Phys. Rev. Lett.* **79**, 1459–1463.
Reinhard, D., Hall, B. D., Ugarte, D. & Monot, R. (1997). *Phys. Rev. B*, **55**, 7868–7881.
Warren, B. E. (1990). *X-ray Diffraction.* New York: Dover.

Waser, J. & Schomaker, V. (1953). *Rev. Mod. Phys.* **25**, 671–690.
Whetten, R. L., Khoury, J. T., Alvarez, M. M., Murthy, S., Vezmar, I., Wang, Z. L., Stephens, P. W., Cleveland, C. L., Luedtke, W. D. & Landman, U. (1996). *Adv. Mater.* **8**, 428–433.
Wilson, A. J. C. (1992). Editor. *International Tables for Crystallography*, Vol. *C*. Dordrecht: Kluwer.
Yang, C. Y. (1979). *J. Cryst. Growth*, **47**, 274–282.
Zanchet, D., Hall, B. D. & Ugarte, D. (2000). *J. Chem. Phys. B*. Submitted.